Mixing in an Agitated Tubular Reactor

Jos. J. Derksen*

School of Engineering, University of Aberdeen, Aberdeen, UK

We analyze, through numerical simulations, the single-phase liquid flow and associated passive scalar mixing in a tubular reactor that is agitated by lateral shaking, which induces the motion of a solid mixing element inside the reactor. The Reynolds number associated with the shaking motion is in the range 1200–5600. Dependent on its specific value, we perform direct or large eddy simulations. A fixed-grid lattice-Boltzmann method is used for solving the fluid flow. The moving boundary condition at the surface of the mixing element is dealt with by means of an immersed boundary method. To quantify mixing, a transport equation for a passive scalar is solved in conjunction with the flow dynamics.

Keywords: tubular reactor, mixing, direct and large eddy simulation, scalar transport

INTRODUCTION

A novel type of continuous mixing system is shown in Figure 1. It consists of an outer tube with circular cross section that undergoes a sinusoidal motion in the lateral horizontal direction. This in turn induces the lateral motion and rotation of a solid internal mixing element (called "the internal" in the remainder of this paper) that has the form of a round tube with holes, as depicted in the figure. This through-flow mixing system can be used as a reactor, a blender, as well as a system to promote solid particle suspension and agitation. In this paper we only consider its single-phase operation. The working fluid is a liquid of constant density and viscosity.

The research described in this paper is purely numerical and of an exploratory nature. The aim is to show the feasibility, as well as the limitations, of our numerical approach to solve fluid flow and scalar transport in this geometrically and kinematically complex flow system under transitional and mildly turbulent conditions. Such simulations then will allow us (in future work) to make predictions of the performance of this mixing device under specific process conditions that can be compared with experimental data, as well as with the performance of other continuous flow mixing devices at comparable conditions.

As can be judged from Figure 1, the dimensionality of the parameter space of this mixing device is extensive and contains the frequency and amplitude of the shaking motion, liquid properties, the through-flow rate, gravitational acceleration and the density of the internal, as well as geometrical (i.e. aspect) ratios. Numerical simulations are an effective way to explore, for process design purposes, large parts of the parameter space and we plan to do so in future research. Future research also should involve the assessment of numerical effects, most importantly establishing grid independence, as well as validation by means of experimental data.

This brief paper is organized in the following manner: we will start by defining the flow system and characterizing it in terms of a set of dimensionless numbers. Then, we make a number of simplifying assumptions. Subsequently turbulence treatment and numerical methods are briefly discussed, with referencing to the literature for further details. In the Results section the first part describes flow field results, and the second part passive scalar transport. The paper is closed with a Summary & Conclusions section.

FLOW SYSTEM

The geometrical layout of the agitated tubular reactor is given in Figure 1. The main geometrical parameters are the inner diameter of the outer tube (D) and its length L, as well as the diameter of the internal (D_i). Mixing is enhanced by holes in the cylindrical internal. The placement and diameters of the holes along with further details are provided in Figure 1, which also defines the coordinate system.

The internal has three degrees of freedom, as specified in Figure 2. These are the lateral horizontal location of its centre x_i, its vertical location z_i, and its rotation angle α_i along the y-axis. The internal does not touch the outer tube with its surface. It has spacers that keep a minimum distance equal to ε between the inner surfaces of the outer tube and the outer surface of the internal. The working fluid is Newtonian with kinematic viscosity ν and density ρ. The solid material that the internal is made of has a density of $\rho_s = 8.0\rho$, except for one simulation that has a density ratio of 4.0. The internal feels a net gravity force in the negative z-direction.

The entire system is agitated by shaking it in a sinusoidal way in the x-direction: the displacement has an amplitude A and a frequency f: $A\sin(2\pi f t)$. This shaking induces motion of the internal which in turn induces mixing. When in operation, the mixer has a continuous through-flow in the y-direction with a volumetric flow rate ϕ_V giving rise to a superficial velocity of $U \equiv \frac{4\phi_V}{\pi D^2}$.

The above set of process parameters has been combined to a set of non-dimensional numbers where the length scale is mostly taken as the outer tube diameter D. Other dimensions of the system can be derived from the aspect ratios, as given in Figures 1 and 2. The through-flow Reynolds number is defined as $Re_\phi \equiv \frac{UD}{\nu}$; the shaking motion is characterized by a Reynolds number $Re_s \equiv \frac{2\pi f A D_i}{\nu}$, a Strouhal number $\text{Str} \equiv \frac{fD}{U}$, and the amplitude over diameter ratio A/D. The ratio of shaking inertia
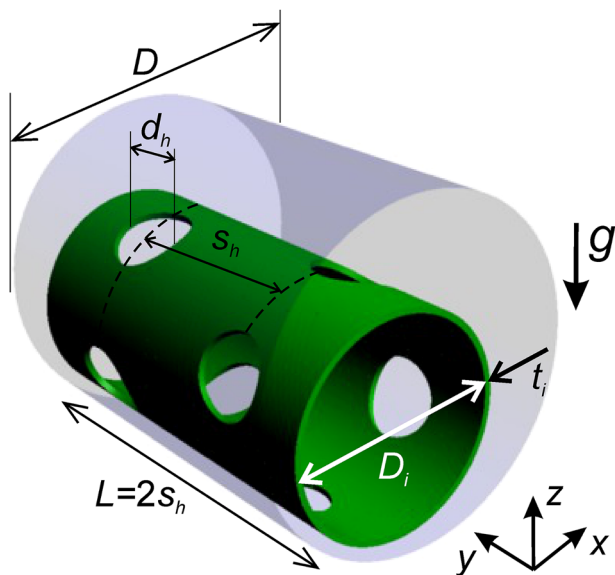
Figure 1. Flow geometry. An internal mixing element (in green) can move inside a tube of diameter D that is shaken in the x-direction. The internal feels a net gravity force that acts in the negative z-direction. The overall flow is in the y-direction; the simulations assume periodic conditions in y-direction. The dimensions as given in the drawing relative to the tube diameter are: $D_i = 0.62D$, $L = 1.28D$, $d_h = 0.25D$, and $t_i = 0.013D$. The origin of the coordinate system is at the centre of the outer tube and at its front.

and net gravity of the internal is expressed as $\theta \equiv \frac{\rho A(2\pi f)^2}{g(\rho_s - \rho)}$. Finally, we have the density ratio ρ_s/ρ.

The simulations are performed in a reference frame that moves with the shaking motion. This implies that an inertial body force is applied to the liquid: $\mathbf{f} = -\rho A(2\pi f)^2 \sin(2\pi ft)\mathbf{e_x}$. Furthermore, we apply periodic conditions in the y-direction. This means that the geometry, as shown in Figure 1, can be seen as a section taken from a much longer mixing system. A major simplification in the
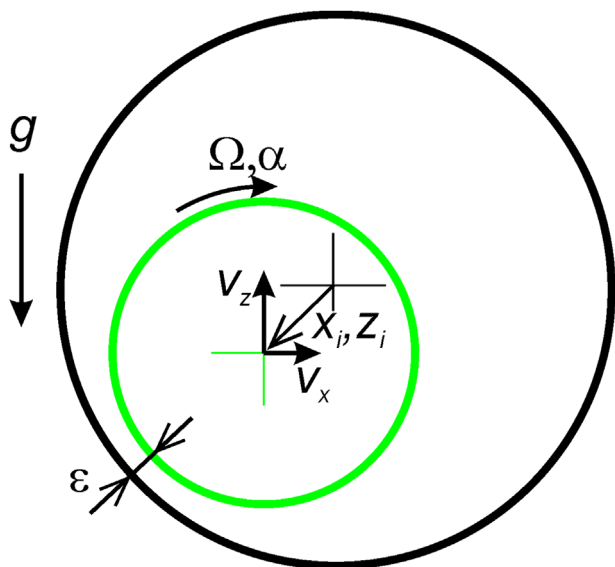
Figure 2. Schematic of the degrees of freedom of the internal (x_i, z_i, and angle α), the associated velocities (v_x, v_z, Ω), and the minimum distance ε between internal and tube; $\varepsilon = 0.038D$.

current study is that we set the volumetric flow rate $\phi_V = 0$. In this case, the mixing is only due to the shaking motion. It also implies that $Re_\phi = 0$ and that the Strouhal number becomes infinite and, in this situation, is not a meaningful dimensionless parameter.

When the distance between the outer surface of the internal and the inner surface of the tube equals ε, the internal collides. In the simulations we have applied two collision models. In the hard model a fully elastic collision is performed and the velocity of the internal changes instantaneously. In the soft model, once the distance ε is reached, an elastic spring is activated that applies a normal repulsive force on the internal proportional to the overlap: $F_s = k(\varepsilon - s)$, with k the spring constant and $s < \varepsilon$ the distance between internal and outer tube. The hard as well as the soft model assume frictionless collisions so that the angular velocity Ω of the internal does not change upon collision.

NUMERICS

The lattice-Boltzmann method has been applied to solve the fluid flow. The specific numerical scheme is due to Somers.[1] The scheme applies a uniform, cubic (edge length Δ) grid with the flow variables defined in the cube centers. Off-grid boundary conditions, such as the no-slip conditions on the tube surface and on the internal, are enforced through an immersed boundary method.[2] These surfaces are represented by a set of closely spaced points (nearest neighbour spacing typically 0.7Δ); for the internal this set of points is shown in Figure 3. At these points, we force the fluid to have the same velocity as the local velocity of the solid surface. The immersed boundary method used is based on interpolation of velocities and extrapolation of forces.[2] Velocities at the immersed boundary points are estimated by interpolation of the surrounding grid velocities; the forces acting on the fluid at the immersed boundary points are extrapolated to the surrounding grid nodes. Integration of the immersed boundary forces over the surface of the internal gives the total hydrodynamic force $\mathbf{F}$ and torque $\mathbf{T}$ on the internal. The x and z component of $\mathbf{F}$ as well as the y component of $\mathbf{T}$ are taken into account when solving the equations of motion of the internal.

In this study, the cubic grid has a resolution such that the tube diameter D spans 156 lattice spacings. This leads to an overall grid node count of approximately 5 M. The number of immersed boundary points on the internal is 270 000; on the outer tube it is 140 000. At this stage of the research, we have not yet considered grid effects and thus are not able to show grid convergence. Time stepping in lattice-Boltzmann methods is largely dictated by constraints on the Mach number.[3] In the simulations presented here, it takes 10 000 time steps to complete one shaking cycle, i.e. $f\Delta t = 1 \cdot 10^{-4}$.

The three equations of motion of the internal (translational in x and z direction, rotational along the y-axis) are solved with a split-derivative method.[4] The forces on the internal are gravity and hydrodynamic force $\mathbf{F}$, as well as the collision force if a soft collision model is applied. The hydrodynamic torque $\mathbf{T}$ on the internal is included in the rotational equation of motion.

In addition to solving the flow and the dynamics of the internal, we have solved the transport of a passive scalar according to a convection-diffusion equation:

$$\frac{\partial c}{\partial t} + \mathbf{u} \cdot \nabla c = \Gamma \nabla^2 c \tag{1}$$

with c the scalar concentration, $\mathbf{u}$ the velocity field that is the result of the lattice-Boltzmann flow solver, and Γ the diffusion
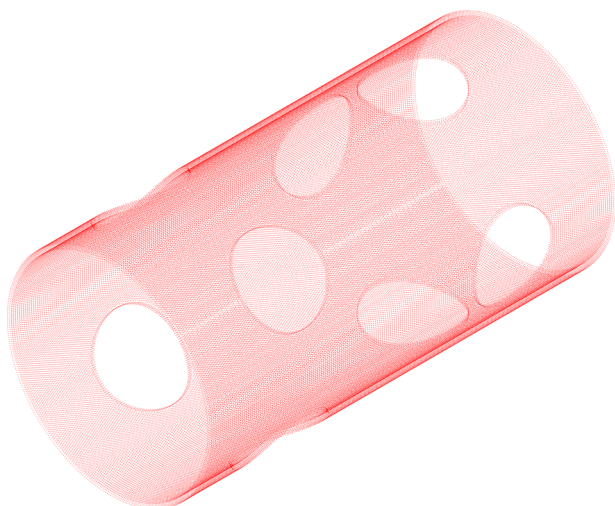
Figure 3. Representation of the internal mixing element by a closely spaced set of points on its surface. The total number of points is approximately 270 000.

coefficient. Equation (1) is discretized according to a finite volume method on the same (uniform, cubic) grid as applied by the lattice-Boltzmann scheme, and explicitly updated in time with the same time step, as used in the lattice-Boltzmann method. We apply flux limiters[5] to suppress false diffusion. In the present work, we set $\Gamma = 0$ so that the (limited) levels of diffusion observed in the simulations are due to the finite resolution of the grid and (still) some numerical diffusion. Procedures similar to the ones proposed in our previous work[6] were used for setting non-penetration boundary conditions at the moving solid surfaces of the internal, as well as for assigning scalar concentrations to grid nodes that are uncovered due to the motion of the internal.
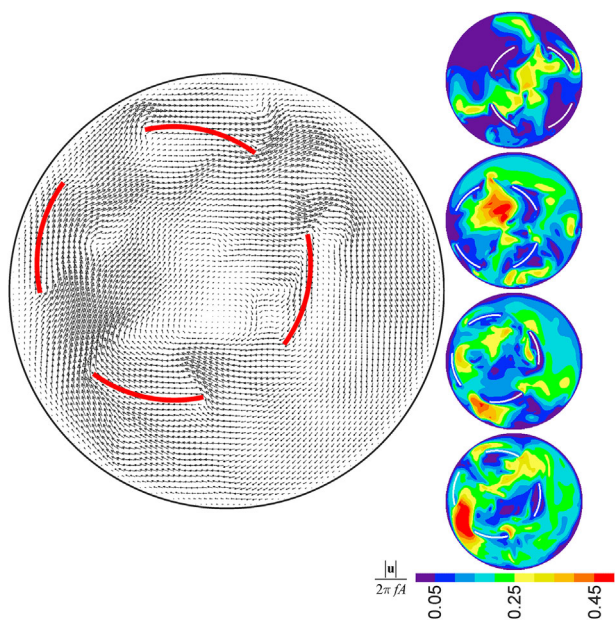
Figure 4. Left: instantaneous velocity vectors in an xz cross section of the flow at $y = L/4$ after the flow is fully developed. Right: impressions of how the flow starts in terms of velocity magnitude contours in the same xz-plane. From top to bottom: $tf = 0.25, 0.5, 1.0, 2.0$. Base-case conditions.
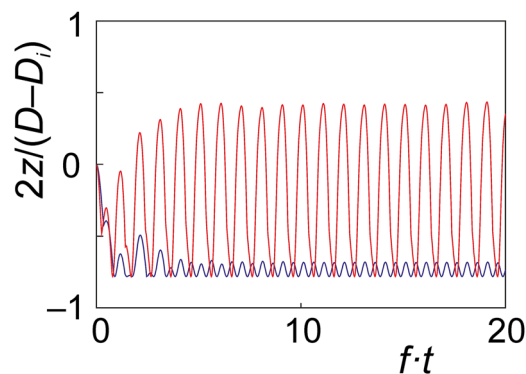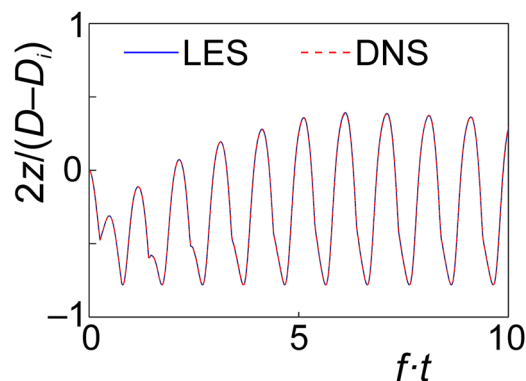

Figure 5. Time series of the vertical (z) coordinate of the centre location of the internal. Red curve: base-case (which has a density ratio $\rho_s/\rho = 8.0$); blue curve: same as base-case except that $\rho_s/\rho = 4.0$.

In this work, the Reynolds numbers associated with the shaking motion (Re_s) were in the range 1200–5600. By default, it was attempted to solve the flow without the use of a turbulence model. Unphysical instabilities occurred when Re_s exceeded approximately 3000. In such situations, we switch to large eddy simulations (LES) and apply a standard Smagorinsky subgrid scale model[7] with a Smagorinsky constant $C_S = 0.1$. In the LES cases, the scalar diffusion coefficient Γ is kept at zero level, i.e. we do not apply a finite level turbulent Schmidt number.
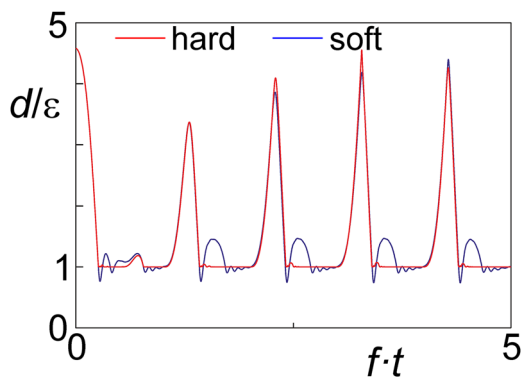
RESULTS

Fluid Flow

A base case has been defined with the following dimensionless parameters: $Re_s = 5{,}600$, $A/D = 1.13$, $\rho_s/\rho = 8.0$, and $\theta = 0.37$, and the geometry as defined in Figures 1 and 2. This case applies hard collisions between internal and outer tube, and a large eddy approach for turbulence modelling. In Figure 4, impressions of the flow field in a xz-cross section passing through four holes in the internal ($y = L/4$) are shown. The shaking motion is started with the internal in the centre of the outer tube ($x_i = z_i = 0$) and fluid at rest ($\mathbf{u} = 0$ everywhere). The velocity magnitude contour plots in Figure 4 illustrate how the flow develops from this initial condition. These and all subsequent images are in the reference frame moving with the shaking motion. Initially ($t = 0.25/f$), the

Figure 6. Time series of the vertical (z) coordinate of the centre location of the internal. Comparison between LES and DNS at $Re_s = 2300$. The rest of the conditions are the same as for the base-case.

Figure 7. Time series reflecting the differences as a result of collision modelling; hard versus soft collisions. The parameter d is the distance of the internal from the wall so that a collision takes place if $d/\varepsilon = 1$. Base-case conditions except that $Re_s = 2300$. DNS flow simulations.

internal moves down due to net gravity and to the right since the shaking motion starts to the left. In the subsequent frames we see an overall increase in the velocity magnitude. The velocity vector plot shows an instantaneous flow field after the system has fully developed. It also gives an impression of the level of resolution of the simulations.

Under base-case conditions, the motion of the internal quickly settles in a periodic state, as can be judged from the time series of the vertical (centre) location of the internal in Figure 5. For an effective operation of this mixing device, inertia of the internal appears important. If we change the density ratio from $\rho_s/\rho = 8.0$ (base-case) to 4.0 and keep all other parameters the same, the internal gets hardly agitated (see the 2nd time series in Figure 5), which has detrimental effects on the mixing performance.

At $Re_s = 2300$, we are able to get stable results without the use of a subgrid-scale model. If we compare these "direct" simulation results with ones obtained with a Smagorinsky subgrid-scale model at the same Reynolds number, we see hardly any difference in the flow field as well as in the levels of agitation of the internal. As an illustration, we show, in Figure 6, very close agreement of the time series of the vertical position of the internal, as obtained

with LES and DNS. These results imply that our procedure is able to represent in a smooth way the transition from laminar to turbulent flow.

Modelling the collisions of the internal is an important aspect of the simulations. In the hard collision model the velocity of the internal changes instantaneously at the moment of the collision. Given the slightly compressible nature of the lattice-Boltzmann scheme,[3] this generates waves in the fluid. These waves are unphysical if the intention is to simulate an incompressible flow. The waves can be avoided by making the collisions "soft" and using an elastic spring, which generates a repulsive force on the internal to push it away from the outer wall. The choice of collision model has some impact on the motion of the internal, as can be seen in Figure 7. The soft model leads to some vibrations of the internal. On average, however, the soft and hard model result in very similar motion of the internal. Without any benchmark or experimental data, it is hard to judge which collision model gives more reliable results. In the remainder of this paper, when discussing scalar transport, results have been generated by using the hard model.

Passive Scalar Transport

In order to directly test the mixing performance of the agitated tubular reactor, the transport equation of a passive scalar concentration c (Equation (1)) was solved in conjunction with the flow dynamics. The initial condition for the simulations involving scalar transport is a fully developed flow field and a segregated scalar concentration field. The latter means that we set $c = 1$ for $z > 0$, and $c = 0$ for $z < 0$.

In Figure 8, impressions of the mixing process are shown for two different Reynolds numbers Re_s. We see the formation of scalar concentration striations and, in the course of time, a homogenization of the concentration field with faster mixing for the higher Reynolds number. To quantify mixing, we define the scalar variance as $\sigma_c \equiv \sqrt{\langle c^2 \rangle - \langle c \rangle^2}/\langle c \rangle$ with $\langle \rangle$ denoting spatial averaging over instantaneous realizations of the concentration field, so that σ_c is a function of time. In Figure 9, we show an example of a σ_c time series where the spatial average is taken over the centre vertical (yz) plane. Given that at time zero the scalar is segregated,
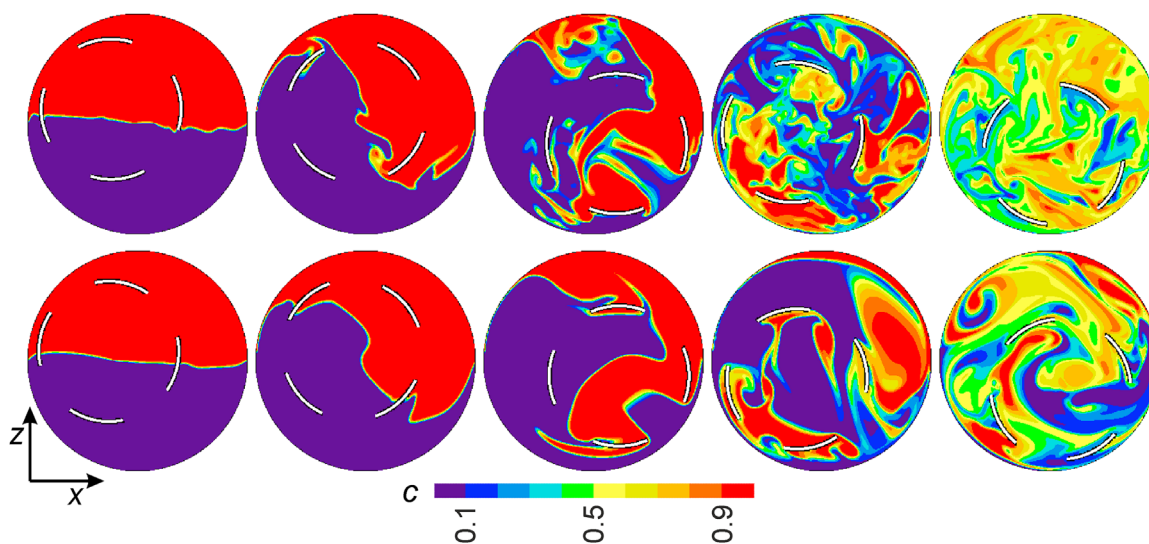
Figure 8. Scalar mixing in the form of concentration contours in the xz-plane at $y = L/4$. Top row: $Re_s = 5600$ (LES); bottom row: $Re_s = 1200$ (DNS). From left to right $tf = 0.02, 0.2, 0.4, 0.8, 1.6$ with at $t = 0$ a fully developed flow and a segregated scalar field.
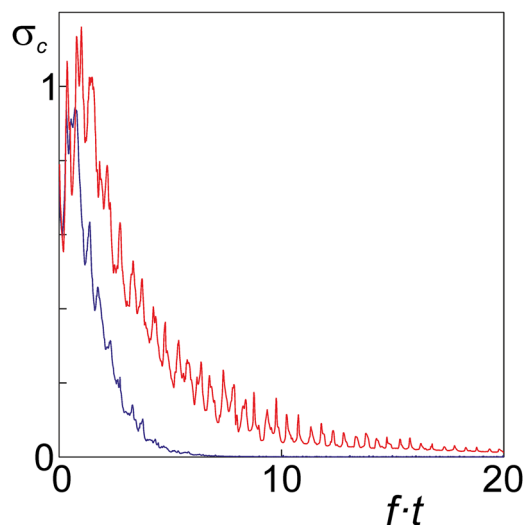
Figure 9. Time series of scalar variance $\sigma_c \equiv \sqrt{\langle c^2 \rangle - \langle c \rangle^2} / \langle c \rangle$ in the yz-plane with $x = 0$ as a function of time for $Re_s = 5600$ (blue curve) and $Re_s = 1200$ (red curve).

REFERENCES

[1] J. A. Somers, *Appl. Sci. Res*. **1993**, *51*, 127.

[2] J. Derksen, H. E. A. Van den Akker, *AIChE J*. **1999**, *45*, 209.

[3] S. Succi, *The Lattice Boltzmann Equation for Fluid Dynamics and Beyond*, Clarendon Press, Oxford **2001**.

[4] O. Shardt, J. J. Derksen, *Int. J. Multiphas. Flow* **2012**, *47*, 25.

[5] P. K. Sweby, *SIAM J. Numer. Anal*. **1984**, *21*, 995.

[6] J. J. Derksen, *AIChE J*. **2008**, *54*, 1741.

[7] J. Smagorinsky, *Mon. Weather Rev*. **1963**, *91*, 99.

the starting value of σ_c is approximately $\frac{1}{2}\sqrt{2}$. We see the decay of scalar variance and it being faster for the higher Reynolds number. If $\sigma_c = 0.02$ is set as the level for a practically homogeneous system, then for $Re_s = 5600$ homogenization is achieved after fewer than 10 shaking periods; for $Re_s = 1200$, it takes at least 15 periods. The periodic fluctuations are due to the periodic motion of the internal.

SUMMARY & CONCLUSIONS

In this paper we have shown the feasibility of performing single-phase flow and mixing simulations of a novel agitated tubular reactor. Simulations so far have been on systems operating in the transitional / early turbulent regime. It was shown that we can make a smooth transition from direct (i.e. no turbulence model) to large eddy simulations. The simulation procedure is able to apply a hard as well as a soft model for the collisions of the internal mixing element with the outer tube wall. It was highlighted that the internal mixing element needs sufficient inertia (i.e. mass) to be sufficiently agitated by the shaking motion of the outer tube. Including passive scalar variance calculations allows for directly quantifying the mixing process, for instance in terms of the decay time of scalar variance.

This paper describes a feasibility study so that much more work needs to be done before applying the simulations for reactor design. The next steps are verification (e.g. establishing grid convergence) and validation (e.g. comparison with experimental data). Then we will be including through-flow so that we will see mixing not only due to the motion of the internal, but also due to an average axial velocity. It will be interesting to quantify the relative importance of these two contributions to mixing as a function of operational conditions.

ACKNOWLEDGEMENT